

# Dimension Reduction via Gaussian Ridge Functions

Pranay Seshadri\*    Shaowu Yuchi†    Geoffrey T. Parks‡

May 18, 2022

## Abstract

Ridge functions have recently emerged as a powerful set of ideas for subspace-based dimension reduction. In this paper we begin by drawing parallels between ridge subspaces, sufficient dimension reduction and active subspaces; contrasting between techniques rooted in statistical regression to those rooted in approximation theory. This sets the stage for our new algorithm that approximates what we call a Gaussian ridge function—the posterior mean of a Gaussian process on a dimension reducing subspace—suitable for both regression and approximation problems. To compute this subspace we develop an iterative algorithm that optimizes over the Grassmann manifold to compute the subspace, followed by an optimization of the hyperparameters of the Gaussian process. We demonstrate the utility of the algorithm on an analytical function, where we obtain near exact ridge recovery, and a turbomachinery case study, where we compare the efficacy of our approach with four well known sufficient dimension reduction methods: MAVE, SIR, SAVE, CR. The comparisons motivate the use of the posterior variance as a heuristic for identifying the suitability of a dimension reducing subspace.

## 1 Introduction

Dimension reduction is essential for modern data analysis. Its utility spans both simulation informatics and statistical regression fields. The objective of dimension reduction is to obtain parsimoniously parameterized models—functions of few variables that can be used for predicting, understanding and visualizing the trends observed in high-dimensional data-sets. These data-sets may originate from a tailored *design of experiment* of computer models (see [29]) and

---

\*Research Associate, Department of Engineering, University of Cambridge, U.K., [ps583@cam.ac.uk](mailto:ps583@cam.ac.uk)

†Undergraduate Research Assistant, Department of Engineering, University of Cambridge, U. K.

‡Reader, Department of Engineering, University of Cambridge, U. K.

are therefore deterministic, or they may originate from the observations of sensors and are therefore subject to measurement noise. Across both paradigms, techniques and ideas within *subspace-based dimension reduction* have proven to be extremely fruitful in inference. Application areas that have benefitted from subspace-based dimension reduction range from airfoil aerodynamics [21] and combustion [26] to economic forecasting (see page 4403 in [2]), turbomachinery aerothermodynamics [33], solar energy [9] and epidemiology [15]. To motivate an exposition of the relevant literature and to set the stage for our paper, we introduce the trivariate function  $y = \log(x_1 + x_2 + x_3)$ . In Figure 1, we generate scatter plots of the function on three different subspaces  $\mathbf{k}^T \mathbf{x}$ —i.e., linear combinations of the three variables  $x_1, x_2$  and  $x_3$ . In (a)  $\mathbf{k}$  is one of canonical vectors, in (b) all the elements of  $\mathbf{k}$  are equivalent (and normalized), while in (c) we moderately perturb the entries in (b). Naturally, we find the subspace  $\mathbf{k}^T \mathbf{x}$  in (b) to be *optimal* in the sense that it most accurately characterizes the 3D function as a function of one variable. Scatter plots of the kind in Figure 1 where the horizontal axis is a subspace of the inputs are known as *sufficient summary plots* [11]. These plots are useful in identifying low-dimensional structure in high dimensional problems. However, as the selection of  $\mathbf{k}$  in Figure 1 illustrates, the impediment to realizing this identification is an appropriate choice of the subspace.

Enter *active subspaces* [6], a collection of ideas that facilitate subspace-based dimension reduction for deterministic computer models. If one can compute gradients of a function  $f$ , or even approximate them, then one can identify directions along which (on average)  $f$  exhibits the greatest variation, and conversely directions along which (on average)  $f$  is near constant<sup>1</sup>. Active subspaces owes its development to initial work by Samarov [32] and more recent work by Constantine et al. (see [5, 7, 6]). The latter references build the theory of active subspaces and also offer practical algorithms for their computation. Parallels between active subspaces and *ridge functions* have also been recently explored in literature [8].

The topic of ridge functions [27] may be interpreted as a broad generalization of ideas within active subspaces. They are of the form  $f(\mathbf{x}) = g(\mathbf{M}^T \mathbf{x})$  where  $\mathbf{M}$  is a tall matrix, implying that  $g$  is a function of fewer variables than  $f$ . The elements of  $\mathbf{M}$  and the function  $g$  are useful in identifying low-dimensional structures, in a similar vein as the example discussed above. In the case where  $\mathbf{M}$  is a vector, which implies that  $g$  is univariate function, Cohen et al. [4] provide estimates on how well  $f$  can be approximated using only point evaluations. Building on their work, Fornasier et al. [17] study the case where  $\mathbf{M}$  is a matrix and provide two randomized algorithms for approximating  $g(\mathbf{M}^T \mathbf{x})$ . The work of Tyagi and Cevher [35] is also similar in scope; they provide an algorithm that approximates functions of the form  $f(\mathbf{x}) = \sum_{i=1}^n g_i(\mathbf{M}_i^T \mathbf{x})$ . Clearly, there are similarities between ridge functions, projection pursuit regression (see page 390 in [18]) and by association, single layer neural networks. However, there are

<sup>1</sup>Assuming of course  $f$  admits an active subspace; there is no guarantee that every differentiable multivariate function  $f$  admits an active subspace

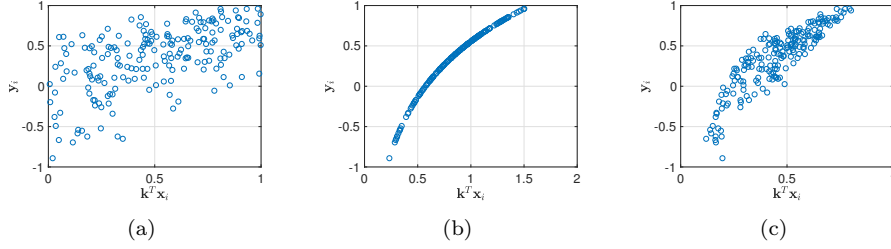


Figure 1: Sufficient summary plots of the function  $y = \log(x_1 + x_2 + x_3)$  where the horizontal axis is given by  $\mathbf{k}^T(x_1, x_2, x_3)$ . In (a)  $\mathbf{k} = (1, 0, 0)^T$ ; in (b)  $\mathbf{k} = (1/\sqrt{3}, 1/\sqrt{3}, 1/\sqrt{3})^T$ , while in (c)  $\mathbf{k} = (0.2, 0.5, 0.2)^T$ .

some key differences between techniques tailored for approximation and those for statistical regression.

In statistical regression, as alluded to previously,  $f(\mathbf{x})$  is not deterministic and therefore has a conditional density that is not a delta function [6]. Furthermore, the joint density of  $\mathbf{x}$  is not known in the regression setting. In comparison, when working with computer models—i.e., in the approximation paradigm—the joint density of  $\mathbf{x}$  is known and often prescribed according to some optimal design of experiment, for example, Latin hypercube sampling, D-optimal design, etc. Lastly, techniques for estimating gradients for unknown regression functions are notoriously expensive in high dimensions. Thus, non-gradient based approaches are sought.

The field of sufficient dimension reduction is rich in ideas for achieving subspace-based dimension reduction within a statistical regression framework. The goal here is to replace the vector of covariates (inputs) with their projection onto a subspace assembled from the space of the covariates themselves [12]. This subspace must be constructed without loss of information based either on the conditional mean, conditional variance or more generally the conditional distribution of the outputs with respect to the inputs. Numerous methods for estimating these subspaces include sliced inverse regression (SIR) [23], sliced average variance estimation (SAVE) [10], minimum average variance estimation (MAVE) [36] and contour regression (CR) [22], to name a few (see [25] for a detailed review).

We now return to the sufficient summary plots in Figure 1. Assume, we did not know the true function  $f(x) = \log(x_1 + x_2 + x_3)$  and that subfigures (a), (b) and (c) were simply the outcome of any one of the aforementioned algorithms. How do we determine that the subspace in (b) is ideally suited for the data? The logic we pursue in the paper is as follows. Assume we utilize Gaussian process regression (see Chapter 2 in [31]) to estimate the mean and standard deviation of the response  $y_i$ , as shown in Figure 2. Then our criterion for selecting  $\mathbf{k}$  in (b) is clear: it reduces the Gaussian process yielded standard deviation. In other words, for the same value of  $\mathbf{x}_i$  there is only one unique  $y_i$ , ensuring that the deviation from the mean is near zero.

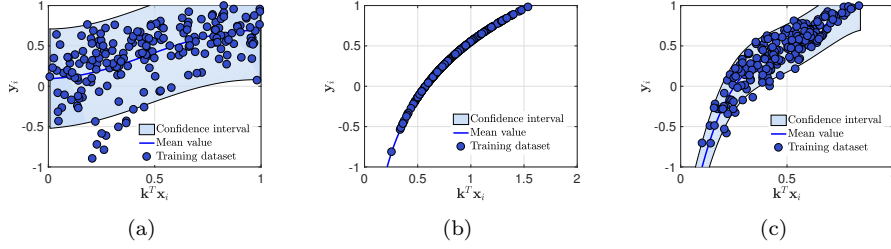


Figure 2: Sufficient summary plots of the function  $y = \log(x_1 + x_2 + x_3)$  where the horizontal axis is given by  $\mathbf{k}^T(x_1, x_2, x_3)$  with a Gaussian process regression response surface. In (a)  $\mathbf{k} = (1, 0, 0)^T$ ; in (b)  $\mathbf{k} = (1/\sqrt{3}, 1/\sqrt{3}, 1/\sqrt{3})^T$ , while in (c)  $\mathbf{k} = (0.2, 0.5, 0.2)^T$ .

There are two key ideas that emerge from this discussion. The first is that the posterior mean of a Gaussian process computed on a dimension reducing subspace is a good candidate for  $g$ . In fact this idea has been previously studied in [34] and [24], albeit using different techniques than those presented here. The second idea is that the suitability of a dimension reducing subspace is reflected by the posterior variance: should the posterior variance be too large, as in Figure 2(a), then one may need to opt for a different choice in  $\mathbf{k}$ .

In a nutshell, our objective in this paper is to offer an algorithm for computing a dimension reducing subspace, under the constraint that  $g$  is the posterior mean of a Gaussian process on this subspace. The remainder of this paper is structured as follows. In section 2 we survey the connections between ridge, active and sufficient dimension reduction subspaces. Then, motivated by the techniques in [34] and [8] we introduce an algorithm for computing a ridge subspace that uses tools from Gaussian process regression and manifold optimization. This is followed by numerical examples in 4.

## 2 Ridge functions

If there exists a function  $f : \mathbb{R}^d \rightarrow \mathbb{R}$  and a matrix  $\mathbf{M} \in \mathbb{R}^{d \times m}$ , with  $m \leq d$ , that satisfies

$$f(\mathbf{x}) = g(\mathbf{M}^T \mathbf{x}), \quad (1)$$

for a function  $g : \mathbb{R}^m \rightarrow \mathbb{R}$ , then  $f$  is a *ridge function* [27]. We call the subspace associated with the span of  $\mathbf{M}$  its *ridge subspace*, denoted by  $\mathcal{S}(\mathbf{M})$ . We also assume that the columns of  $\mathbf{M}$  are orthonormal, i.e.,  $\mathbf{M}^T \mathbf{M} = \mathbf{I}$ . The above definitions imply that the gradient of  $f$  is zero along directions that are orthogonal to  $\mathcal{S}(\mathbf{M})$ . In other words, if we replace  $\mathbf{x}$  with  $\mathbf{x} + \mathbf{h}$  where  $\mathbf{M}^T \mathbf{h} = 0$ , then it is trivial to see that  $f(\mathbf{x} + \mathbf{h}) = g(\mathbf{M}^T(\mathbf{x} + \mathbf{h})) = f(\mathbf{x})$ .

## 2.1 Computing the optimal subspace

So given point evaluations of  $f$  how does one compute  $\mathbf{M}$ ? Also, what are the properties of  $\mathbf{M}$ ? In their paper, Constantine et al. [8] draw our attention to the conditional and marginal densities defined on the subspace coordinates of the ridge subspace and its orthogonal complement. There are two main ideas they present.

The first is the *orthogonal invariance* associated with  $\mathbf{M}$ , i.e. we are not interested in estimating a particular  $\mathbf{M}$ , but rather the subspace of  $\mathbf{M}$ —i.e., the ridge subspace. To study this further, we place a few additional assumptions on 1. Let the joint probability density function  $\rho(\mathbf{x})$  and marginal densities  $\rho_i$  related by

$$\rho(\mathbf{x}) = \prod_{i=1}^d \rho(x^{(d)}). \quad (2)$$

We assume that  $f$  is square integrable with respect to this probability density function

$$\int_{\rho} f^2(\mathbf{x}) \rho(\mathbf{x}) d\mathbf{x} < \infty, \quad (3)$$

where the domain of  $f$  is the support of  $\rho$ . Define  $\mathcal{S}(\mathbf{N})$  to be the orthogonal complement of the ridge subspace, where

$$\mathbf{N} = (\text{null}(\mathbf{M}^T)) \quad \text{with} \quad \mathbf{N} \in \mathbb{R}^{d \times m-d}. \quad (4)$$

Placing the columns of  $\mathbf{M}$  and  $\mathbf{N}$  together in a single matrix

$$\mathbf{G} = [\mathbf{M} \quad \mathbf{N}], \quad (5)$$

readily implies that  $\mathbf{G}\mathbf{G}^T = \mathbf{I}$ . We now write the full decomposition of the  $f$  as

$$f(\mathbf{x}) = f(\mathbf{G}\mathbf{G}^T \mathbf{x}) = f(\mathbf{M}\mathbf{M}^T \mathbf{x} + \mathbf{N}\mathbf{N}^T \mathbf{x}) = f(\mathbf{M}\mathbf{u} + \mathbf{N}\mathbf{v}), \quad (6)$$

with the following subspace coordinates

$$\mathbf{u} \in \mathbb{R}^m \quad \text{and} \quad \mathbf{v} \in \mathbb{R}^{d-m}, \quad (7)$$

where

$$\mathbf{u} = \mathbf{M}^T \mathbf{x} \quad \text{and} \quad \mathbf{v} = \mathbf{N}^T \mathbf{x}. \quad (8)$$

It should be noted here that if  $f$  admits a ridge function structure, then the gradient of  $f$  along the directions  $\mathbf{N}\mathbf{v}$  are expected to be zero.

For a fixed subspace coordinate  $\mathbf{u}$ , Constantine et al. write the conditional expectation of  $f$  to be

$$\mathbb{E}(f|\mathbf{u}, \mathbf{M}) = \int f(\mathbf{M}\mathbf{u} + \mathbf{N}\mathbf{v}) \pi(\mathbf{v}|\mathbf{u}) d\mathbf{v} \quad (9)$$

where the conditional probability  $\pi(\mathbf{v}|\mathbf{u})$  can be expressed in terms of its marginal  $\pi(\mathbf{u})$  and  $\pi(\mathbf{u}, \mathbf{v})$  joint probabilities

$$\pi(\mathbf{v}|\mathbf{u}) = \frac{\pi(\mathbf{u}, \mathbf{v})}{\pi(\mathbf{u})} = \frac{\rho(\mathbf{M}\mathbf{u} + \mathbf{N}\mathbf{v})}{\int \rho(\mathbf{M}\mathbf{u} + \mathbf{N}\mathbf{v}) d\mathbf{v}}. \quad (10)$$

To demonstrate the orthogonal invariance associated with  $\mathbf{M}$  we replace it with  $\mathbf{M}\mathbf{Q}$  where  $\mathbf{Q} \in \mathbb{R}^{m \times m}$  is an orthogonal matrix. Plugging this into (9) yields

$$\mathbb{E}(f|\mathbf{u}, \mathbf{M}\mathbf{Q}) = \int f(\mathbf{M}\mathbf{Q}(\mathbf{Q}\mathbf{M})^T \mathbf{x} + \mathbf{N}\mathbf{v}) \pi(\mathbf{v}|\mathbf{u}) d\mathbf{v} \quad (11)$$

$$= \int f\left(\mathbf{M} \underbrace{\mathbf{Q}^T \mathbf{Q}}_{\mathbf{I}} \mathbf{M}\mathbf{x} + \mathbf{N}\mathbf{v}\right) \pi(\mathbf{v}|\mathbf{u}) d\mathbf{v} \quad (12)$$

$$= \int f(\mathbf{M}\mathbf{u} + \mathbf{N}\mathbf{v}) \pi(\mathbf{v}|\mathbf{u}) d\mathbf{v}. \quad (13)$$

It can be easily shown that the conditional probability also remains the same under the orthogonal transformation  $\mathbf{M}\mathbf{Q}$ . This demonstrates that the particular choice of  $\mathbf{M}$  does not matter, but rather its subspace does. In [8], the authors draw our attention to Theorem 8.3 in Pinkus [27], which proves that  $\mathbb{E}(f|\mathbf{u}, \mathbf{M})$  is the *optimal* ridge subspace in the  $l_2$  norm.

So how do we compute this *optimal subspace*? The second point made in [8] is that this subspace can be computed by solving the following quadratic form

$$\begin{aligned} \underset{\mathbf{M}}{\text{minimize}} \quad & \omega(\mathbf{M}) = \frac{1}{2} \int_{\rho} (f(\mathbf{x}) - \mathbb{E}(f|\mathbf{u}, \mathbf{M}))^2 \rho(\mathbf{x}) d\mathbf{x} \\ \text{subject to} \quad & \mathbf{M} \in \mathbb{G}(m, d). \end{aligned} \quad (14)$$

The constraint in (14) restricts  $\mathbf{M}$  to be from the subspace  $\mathbb{G}(m, d)$ , which denotes the space of  $m$ -dimensional subspaces of  $\mathbb{R}^d$  i.e., the Grassman manifold (see page 30 in [1]). Readers will note that while similar in many respects, the Grassman manifold differs from the *Stiefel* manifold (see page 23 in [1]), defined as the set of all  $d \times m$  matrices with full column rank.

Recognizing (14) as a manifold optimization problem permits us to compute the gradients on the Grassman manifold. Following page 321 in [16], and denoting the gradient on the Grassman by the symbol  $\bar{\nabla}$ , we have

$$\bar{\nabla} \omega(\mathbf{M}) = \int_{\rho} (f(\mathbf{x}) - \mathbb{E}(f|\mathbf{u}, \mathbf{M})) (-\bar{\nabla} \mathbb{E}(f|\mathbf{u}, \mathbf{M})) \rho(\mathbf{x}) d\mathbf{x} \quad (15)$$

$$= \int_{\rho} (\mathbb{E}(f|\mathbf{u}, \mathbf{M}) - f(\mathbf{x})) (\mathbf{I} - \mathbf{M}\mathbf{M}^T) \frac{\partial}{\partial \mathbf{M}} \mathbb{E}(f|\mathbf{u}, \mathbf{M}) \rho(\mathbf{x}) d\mathbf{x}. \quad (16)$$

A few remarks regarding this optimization problem are in order. First, provided the gradients  $\frac{\partial}{\partial \mathbf{M}} \mathbb{E}(f|\mathbf{u}, \mathbf{M}^T) \in \mathbb{R}^{m \times d}$  can be determined, solutions to this optimization problem can be computed using an appropriate gradient based optimizer. In 3.3 we use tools from Gaussian processes to estimate these gradients. Second, (14) is not necessarily convex, therefore we are not guaranteed a unique global minimizer during an optimization. However, as we demonstrate in our section 4, near optimal solutions can be computed.

## 2.2 Connections between ridge subspaces and sufficient dimension reduction

One approach to estimate the ridge subspace is to develop a computational method that implements (14). In section 3.2 we detail such a procedure using Gaussian process regression. However, other algorithms that utilize ideas from sufficient dimension reduction theory can also be leveraged. The key is to understand the relationship between the subspace computed from techniques like SIR, SAVE and CR and the *ridge subspace*. As a prelude to exploring these connections, it is important to distinguish statistical regression from approximation.

In the regression setting we are given independent and identically distributed random variables  $(\mathbf{x}_i, y_i)$  from an *unknown* joint distribution  $\pi(\mathbf{x}, y)$ , where  $i = 1, \dots, N$  for some  $N$ . Our objective is to characterize the conditional dependence of  $y$  on  $\mathbf{x}$  either through its expectation  $\mathbb{E}(y|\mathbf{x})$  or its variance  $\sigma^2(y|\mathbf{x})$ . This requires a model  $y = h(\mathbf{x}_i) + \epsilon$  for predicting  $y$  given  $\mathbf{x}$ , where  $\epsilon$  is a zero-mean random error that is independent of  $\mathbf{x}$ . This implies that for the same  $\mathbf{x}_*$  we have multiple values if  $y_*$ . The function  $h$  here may be either parametric (e.g., polynomial least squares) or semi-parametric (e.g., Gaussian process regression) and will typically be obtained by penalizing the errors in prediction via an appropriate *loss function*; the most common one being the  $l_2$  norm error [18]. In the approximation setting, we are given input / output pairs  $(\mathbf{x}_i, y_i)$  obtained by evaluating a computer model under a known density  $\pi(\mathbf{x})$  via an appropriately chosen *design of experiment*. These inputs may be either design variables, boundary conditions or state variables. As the computer model does not have any random error associated with it, multiple evaluations for a particular  $\mathbf{x}_*$  will always yield the same  $y_*$ . In this context, our objective is to obtain a useful approximation  $y = f(\mathbf{x})$  valid for *all*  $\mathbf{x}$  over  $\pi(\mathbf{x})$ .

Now, despite these differences, ideas from sufficient dimension reduction can be used for approximation. Glaws et al. [19] detail the mathematical nuances involved in doing so for SIR and SAVE. They prove that the conditional independence of the inputs and outputs in the approximation setting—i.e., for a deterministic function—is equivalent to the function being a ridge function (see Theorem 6 in [19]). But is there any benefit in using SIR, SAVE and other sufficient dimension reduction methods for dimension reduction when approximating? Adraghi and Cook [2] suggest that moment-based sufficient dimension reduction techniques such as SIR and SAVE, which are designed to provide estimates of the minimum sufficient linear reduction, are not tailored for prediction. They further suggest that model-based inverse regression techniques, such as those presented in [13] may be more useful. In section 4 we test their suggestion by comparing the results of our proposed algorithm with SIR, SAVE, MAVE and CR.

## 2.3 Connections between ridge subspaces and active subspaces

Active subspaces [6] refer to a set of ideas for parameter-based dimension reduction in the *approximation* setting (see 2.2). To compute the active subspace of a function  $f$ , we require that  $f$  be differentiable and Lipschitz continuous—implying that the norm of its gradient  $\nabla f_{\mathbf{x}}$  is bounded. Then one assembles the covariance matrix  $\mathbf{C}$

$$\mathbf{C} = \int \nabla f_{\mathbf{x}} \nabla f_{\mathbf{x}}^T \rho(\mathbf{x}) d\mathbf{x} \quad (17)$$

also known as the outer product of the gradient matrix<sup>2</sup>. What follows is a singular value decomposition of  $\mathbf{C}$ , where the first  $m$  eigenvectors are used to define the *active* and remaining  $d-m$  the *inactive* subspaces; the theorem below connects active subspaces and ridge subspaces.

**Theorem 1** *If we assume that  $\mathbf{C}$  admits the eigendecomposition*

$$\mathbf{C} = \begin{bmatrix} \mathbf{M} & \mathbf{N} \end{bmatrix} \begin{bmatrix} \mathbf{\Lambda}_1 & \\ & \mathbf{\Lambda}_2 \end{bmatrix} \begin{bmatrix} \mathbf{M} & \mathbf{N} \end{bmatrix}^T \quad \text{where } \mathbf{\Lambda}_1 \in \mathbb{R}^{m \times m}, \quad (18)$$

then

$$\left( \int (f(\mathbf{x}) - \mathbb{E}(f|\mathbf{M}^T \mathbf{x}))^2 \rho(\mathbf{x}) d\mathbf{x} \right)^{\frac{1}{2}} \leq C (\text{trace}(\mathbf{\Lambda}_2))^{\frac{1}{2}}, \quad (19)$$

where  $C$  is a constant that depends on  $\rho(\mathbf{x})$ .

The proof follows from Theorem 4.4 in [6]. It is important to emphasize that in practice, the right hand side of 19 is difficult to compute because we do not have access to the eigenvalues associated with the covariance matrix that yields eigenvectors  $[\mathbf{M}, \mathbf{N}]$ . Furthermore, while the decay in the eigenvalues above can be used to set the size of  $m$  when using active subspaces, when approximating ridge subspaces, one has to opt for other criterion—for instance, the authors in [34] utilize a Bayesian information criterion to determine  $m$ .

## 3 Gaussian processes

The definition of a Gaussian process is a “collection of random variables, any finite number of which have a joint Gaussian distribution” [31]. It is completely defined by its mean and covariance functions. Restating the definition in the form we need, we have

$$f(\mathbf{x}) \sim \mathcal{GP}(\mu(\mathbf{u}), \mathbf{k}(\mathbf{u})), \quad (20)$$

where  $\mu$  is the mean function and  $\mathbf{k}$  represents a parameterized covariance matrix, albeit with a slight abuse of notation. It is important to note that we define our Gaussian process on the reduced coordinates  $\mathbf{u} = \mathbf{M}^T \mathbf{x}$ . As a result,

---

<sup>2</sup>Note that this is a symmetric positive semidefinite matrix



the computation of the Gaussian process itself does not become prohibitive. In this section we have two main goals. First, to define a Gaussian ridge function and to outline its properties. Second, to provide an algorithm that computes a Gaussian ridge function. To ease our exposition, we assume the existence of a set of  $N$  input/output *training data* pairs  $(\hat{\mathbf{x}}_i, \hat{f}_i)$  for  $i = 1, \dots, N$ ; the superscript  $\hat{\cdot}$  is used for identifying the training data pairs. We then define the following quantities

$$\hat{\mathbf{f}} = \begin{pmatrix} \hat{f}_1 \\ \vdots \\ \hat{f}_N \end{pmatrix}, \quad \hat{\mathbf{U}} = (\hat{\mathbf{u}}_1, \dots, \hat{\mathbf{u}}_N)^T \quad \text{and} \quad \hat{\mathbf{u}}_i = \mathbf{M}^T \hat{\mathbf{x}}_i. \quad (21)$$

For convenience, we also define

$$\tilde{\mathbf{U}} = (\mathbf{u} - \hat{\mathbf{u}}_1, \dots, \mathbf{u} - \hat{\mathbf{u}}_N)^T, \quad (22)$$

where the variable  $\mathbf{u}$  represents a given test point.

### 3.1 Gaussian ridge functions (posterior mean)

Succinctly stated, a Gaussian ridge function is the posterior mean of the Gaussian process in (20), written as

$$\bar{g}(\mathbf{u}) = \mathbf{k}(\mathbf{u}, \hat{\mathbf{U}}) \boldsymbol{\beta}. \quad (23)$$

It is a linear sum of kernel functions with coefficients  $\boldsymbol{\beta}$ —an outcome of the representer theorem (see page 132 of [31]). Before we define these coefficients, we first focus on the covariance term on the right hand side in (23). In what follows we employ the squared exponential covariance kernel

$$k(\mathbf{u}_i, \mathbf{u}_j) = \sigma_f^2 \exp\left(-\frac{1}{2}(\mathbf{u}_i - \mathbf{u}_j)^T \boldsymbol{\Gamma}^{-1}(\mathbf{u}_i - \mathbf{u}_j)\right), \quad (24)$$

where the diagonal matrix  $\boldsymbol{\Gamma}$  is given by

$$\boldsymbol{\Gamma} = \begin{bmatrix} l_1^2 & & 0 \\ & \ddots & \\ 0 & & l_m^2 \end{bmatrix}. \quad (25)$$

The constant  $\sigma_f$  is known as the *signal variance* and constants  $l_1, \dots, l_m$  are the *correlation lengths* along each of the  $m$ -coordinates of  $\mathbf{u}$ . The parameterized covariance matrix  $\mathbf{k}(\mathbf{u}, \hat{\mathbf{U}}) \in \mathbb{R}^{1 \times N}$  in (23) can now be written as

$$\mathbf{k}(\mathbf{u}, \hat{\mathbf{U}}) = (k(\mathbf{u}, \hat{\mathbf{u}}_1), \dots, k(\mathbf{u}, \hat{\mathbf{u}}_N)). \quad (26)$$

The vector of coefficients  $\boldsymbol{\beta} \in \mathbb{R}^N$  is given by

$$\boldsymbol{\beta} = (\mathbf{K} + \sigma_n \mathbf{I})^{-1} \hat{\mathbf{f}}, \quad (27)$$

where the  $(i, j)$ -th entry of the matrix  $\mathbf{K} \in \mathbb{R}^{N \times N}$  is given by

$$\mathbf{K}(i, j) = k(\hat{\mathbf{u}}_i, \hat{\mathbf{u}}_j), \quad (28)$$

in other words it depends only on the training data set. This permits us to write the gradient of the Gaussian ridge function

$$\begin{aligned} \frac{\partial \bar{g}}{\partial \mathbf{u}} &= \frac{\partial \mathbf{k}(\mathbf{u}, \hat{\mathbf{U}})}{\partial \mathbf{u}} \boldsymbol{\beta} \\ &= -\mathbf{\Gamma}^{-1} \tilde{\mathbf{U}} \left( \mathbf{k}(\mathbf{u}, \hat{\mathbf{U}})^T \odot \boldsymbol{\beta} \right), \end{aligned} \quad (29)$$

where the symbol  $\odot$  indicates an element-wise product. In practice, any differentiable kernel may be used to compute the gradient of the Gaussian ridge function. Now, in using a Gaussian ridge function we make two key assertions. First, the Gaussian ridge function is approximately the expectation of  $f$  projected on  $\mathbf{u} = \mathbf{M}^T \mathbf{x}$ , i.e.,

$$\mathbb{E}(f|\mathbf{u}, \mathbf{M}) \approx \bar{g}(\mathbf{u}). \quad (30)$$

As a consequence, its gradients (in (16), see last term on the right hand side), can be computed via

$$\begin{aligned} \frac{\partial}{\partial \mathbf{M}} \mathbb{E}(f|\mathbf{u}, \mathbf{M}) &\approx \frac{\partial \bar{g}}{\partial \mathbf{u}} \frac{\partial (\mathbf{M}^T \mathbf{x})}{\partial \mathbf{M}} \\ &\approx -\mathbf{\Gamma}^{-1} \tilde{\mathbf{U}} \left( \mathbf{k}(\mathbf{u}, \hat{\mathbf{U}})^T \odot \boldsymbol{\beta} \right) \mathbf{x}. \end{aligned} \quad (31)$$

It is clear that the quality of our approximation in (30) is contingent upon a suitable choice of the hyperparameters

$$\boldsymbol{\theta} = \{\sigma_f^2, \sigma_n^2, l_1, \dots, l_m\}. \quad (32)$$

A well-worn heuristic to estimate these hyperparameters, which in itself is a non-convex optimization problem, is to maximize the marginal likelihood (see page 113 [31])

$$\begin{aligned} &\underset{\boldsymbol{\theta}}{\text{maximize}} \quad \log p(\mathbf{u}, \boldsymbol{\theta}) \\ &\text{subject to} \quad \log p(\mathbf{u}, \boldsymbol{\theta}) = -\frac{1}{2} \mathbf{f}^T (\mathbf{K} + \sigma_n^2 \mathbf{I})^{-1} \mathbf{f} - \frac{1}{2} \log |\mathbf{K} + \sigma_n^2 \mathbf{I}| - \frac{N}{2} \log(2\pi). \end{aligned} \quad (33)$$

The first term in  $\log p(\mathbf{u}, \boldsymbol{\theta})$  which depends solely on the covariance matrix and values of  $f$  is the *data-fit* term. The second term, which depends only upon the covariance function is known as the *complexity penalty*, while the third term is simply a normalizing constant. The problem of computing the maximum in (33) can be readily solved via a gradient based optimizer; formulas for the gradients of  $\log p$  with respect to the hyperparameters are given in section 5.9 of [31].

### 3.2 The utility of the posterior variance

In our presentation of Gaussian ridge functions so far we have not discussed the posterior variance. For a fixed coordinate, this posterior variance is a Gaussian distribution with a known mean and variance. However, in practice, there is no reason for this posterior variance to admit a Gaussian distribution. This quantity, given by

$$\mathbb{V}[g(\mathbf{u})] = k(\mathbf{u}, \mathbf{u}) - k(\mathbf{u}, \hat{\mathbf{U}})^T (\mathbf{K} + \sigma_n^2 \mathbf{I})^{-1} \mathbf{k}(\mathbf{u}, \hat{\mathbf{U}}) \quad (34)$$

can be very useful in quantifying the suitability of a particular choice of  $\mathbf{M}$ . Recall, the plots in Figures 1 and 2. Our perception of a successful dimension reduction strategy through a sufficient summary plot is intimately tied to the variance in  $f$  for a fixed coordinate in the dimension reducing subspace. Here we argue that the expectation of the posterior variance  $\mathbb{E}[\mathbb{V}(g)]$ , can be used to gauge the overall effectiveness of the subspace approximant  $\tilde{\mathbf{M}}$ .

We make the above argument for two reasons. First, different dimension reduction methods—tailored for the same projection  $\mathbb{R}^d \rightarrow \mathbb{R}^m$ —will likely yield different subspaces. In Cook and Li [14] a clear distinction is made between dimension reduction techniques that identify a *central subspace* from those that find a *central mean subspace*; an algorithm for computing the *central variance subspace* is introduced in Zhu and Zhu [37]. Our hypothesis is that regardless of the subspace sought, to infer the suitability of a particular  $\hat{\mathbf{M}}$  as a ridge subspace we must be able to compare different methods that by definition will yield different subspaces. To this end, while a metric based on the subspace angle  $\phi$  (see page 329 of [20] and )—i.e.,

$$\begin{aligned} \text{dist}(\mathbf{M}, \tilde{\mathbf{M}}) &= \|\mathbf{M}\mathbf{M}^T - \tilde{\mathbf{M}}\tilde{\mathbf{M}}^T\|_2, \\ &= \sin(\phi) \end{aligned} \quad (35)$$

—is useful for comparing the *distance* between the *ridge subspace*  $\mathbf{M}$  and its approximant  $\tilde{\mathbf{M}}$ , it is limited to comparisons with one technique / subspace. The second point we articulate concerns cases when  $m \geq 3$ , where it is difficult to visually perceive how suitable a choice of  $\tilde{g}$  is. Here, the measure  $\mathbb{E}[\mathbb{V}(g)]$  can be used to (i) quantify the error in the approximation; and (ii) to guide further computer simulations.

### 3.3 Computing the Gaussian ridge via manifold optimization

We now detail our algorithm for estimating  $\mathbf{M}$  using a Gaussian ridge function. It is an iterative approach—optimizing over the Grassmann manifold for estimating  $\mathbf{M}$  and then over the space of the hyperparameters for determining  $\boldsymbol{\theta}$ . Our algorithmic workflow is given below.

First, the data set must be split into a training and testing data set, where the former has  $H$  input/output pairs while the latter has  $N - H$  pairs. For a

given value of  $N$  it is difficult to provide heuristics on what value to set for  $H$ . We report the results of a few different  $H/N$  ratios in Section 4. However, we do require that both testing and training sets are distributed with respect to the measure  $\rho(\mathbf{x})$ .

For our algorithm, we require an initial choice of the ridge  $\mathbf{M}$ ; readily computed by applying a QR factorization on a random matrix and then taking the first  $m$  columns of  $\mathbf{Q}$  (see line 4). This trick ensures that the columns of  $\mathbf{M}$  are orthogonal. It also implies that each call of our algorithm will yield a different result, by virtue of the fact that the initial starting point—i.e.,  $\mathbf{M}_0$ —is different. Following this, it is easy to project the  $d$ -dimensional data  $\mathbf{x}$  to the  $m$ -dimensional space (line 7).

---

**Algorithm 1** Gaussian ridge function approximation

---

**Data:** Input/output pairs  $(\mathbf{x}_i, f_i)$  where  $i = 1, \dots, N$

**Result:** Ridge subspace  $\mathbf{M}$

1 Split the data into training data set:

$$(\hat{\mathbf{x}}_i, \hat{f}_i) \text{ where } i = 1, \dots, H$$

2 Assemble the testing data set:

$$(\hat{\mathbf{x}}_i, \hat{f}_i) \text{ where } i = H+1, \dots, N.$$

3 Initialize:

$$\mathbf{A} = \text{rand}(d, m).$$

4 Compute its QR factorization:

$$[\mathbf{Q}, \mathbf{R}] = \text{qr}(\mathbf{A}).$$

5 Initialize:

$$\mathbf{M}_0 = \mathbf{Q}(:, 1:m).$$

6 **while**  $|\Delta r| \leq \epsilon$  **do**

7     Compute:

$$\hat{\mathbf{u}}_i = \mathbf{M}_0^T \hat{\mathbf{x}}_i \text{ and } \hat{\mathbf{u}}_i = \mathbf{M}_0^T \hat{\mathbf{x}}_i.$$

8     Solve the optimization problem using the training data  $(\hat{\mathbf{u}}_i, \hat{\mathbf{f}}_i)$ :

$$\underset{\boldsymbol{\theta}_*}{\text{maximize}} \log p(\hat{\mathbf{u}}, \boldsymbol{\theta}).$$

9     Solve the Grassmann manifold optimization problem using  $\boldsymbol{\theta}_*$  on the testing data:

$$r = \underset{\mathbf{M}_*}{\text{minimize}} \frac{1}{2} \left\| \hat{\mathbf{f}} - g(\mathbf{M}^T \hat{\mathbf{x}}, \boldsymbol{\theta}_*) \right\|_2^2.$$

10     Set:

$$\mathbf{M}_0 = \mathbf{M}_*.$$

11 **end**

---

Next, we train a Gaussian process model using  $(\hat{\mathbf{u}}_i, \hat{\mathbf{f}}_i)$  and solve the optimization problem in (33) (line 8) to obtain the hyperparameters  $\boldsymbol{\theta}$ . These values are then fed back into the Gaussian process posterior mean—i.e., our approximation of  $\mathbb{E}(f|\mathbf{u}, \mathbf{M})$ —for prediction. In line 10 we optimize over the Grassmann manifold to estimate  $\mathbf{M}_*$ . This process is then repeated till the difference in residuals  $|\Delta r|$  between successive iterations is below a chosen value  $\epsilon$ .

## 4 Numerical studies

Our codes for Algorithm 1 can be found at <https://www.github.com/pesesh/GaussianRidges>. The codes are in MATLAB and require the `gpm1` [30] toolbox for Gaussian processes and `manopt` [3], a set of utilities for manifold optimization. For the manifold optimization subroutine in our codes, we utilized the conjugate gradient method for optimizing over the Grassman manifold with a minimum step size of  $1e-12$  and a tolerance in the norm of the gradient of  $1e-15$ .

For optimizing the hyperparameters in our Gaussian process models, we use the in-built (within `gpm1`) conjugate gradient approach based on the Polack-Ribiere method (see [28]). Initial values for all our hyperparameters were set to 1.

### 4.1 A Gaussian ridge function

In this section we study the outcome of the algorithm provided in 3.3 for discovering the ridge subspace associated with the problem

$$f(x) = h(\mathbf{a}^T \mathbf{x}) \quad \text{where } \mathbf{a} \in \mathbb{R}^{d \times 1}, \mathbf{x} \in \mathbb{R}^d \text{ and } h: \mathbb{R} \rightarrow \mathbb{R}, \quad (36)$$

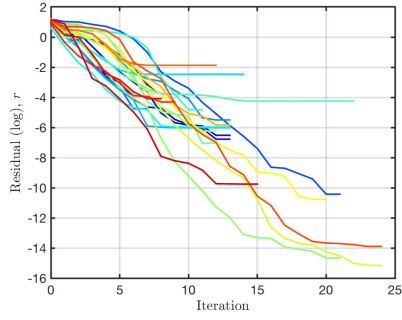
where  $h$  is a univariate Gaussian function with a mean of 0.0 and a standard deviation of 0.07 and where  $\mathbf{a}$  is a normalized random vector. We explore the result of the conjugate gradient optimizer by varying values of  $d$ , the dimensionality associated with  $\mathbf{x}$ , and  $N$ , the number of training and testing points. For all the numerical results, we set both the number of training and testing points to be  $N/2$ ; in full disclosure we have not investigated the effect of varying this ratio.

Figure 3 plots the results for  $d = 5$ . In (a) and (b) we report the convergence histories where the horizontal axis is the number of iterations and the vertical axis is the residual (on a logarithm scale) for  $N = 200$  and  $N = 400$  respectively. Owing to the dependence on the initial value  $\mathbf{M}_0$  (see 3.3), we repeat each optimization 25 times—each shown in a different color. Values of  $\mathbf{M}_0$  are chosen randomly. Sub-figures (c) and (d) show the sufficient summary plots from the *optimized* solutions from the 25 different trials for the two values of  $N$ , i.e.,  $N = 200$  in (c) and  $N = 400$  in (d). Marker colors in sub-figures (c) and (d) are consistent with those in (a) and (b). Similar results for  $d = 100$  are shown in Figure 4 and for  $d = 200$  in Figure 5 for four different values of  $N = [200, 400, 800, 1200]$ .

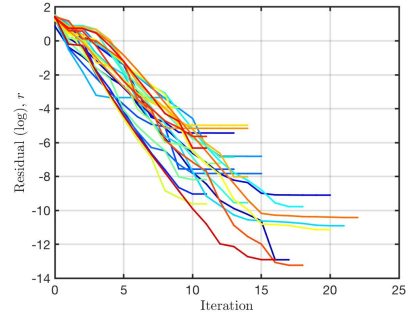
It is clear from the results above that as the total number of testing and training points exceeds a certain value, the conjugate gradient method is able to recover (in some cases to computer precision accuracy) the Gaussian ridge function in (36), even when  $d = 200$ !

But what happens if we corrupt our function with some noise? This represents a departure from the computer model / approximation paradigm, where for the same value of  $\mathbf{x}$  we are guaranteed the same value of  $h(\mathbf{a}^T \mathbf{x})$ . We now consider a problem of the form

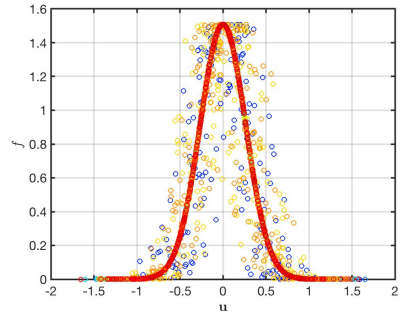
$$f(x) = h(\mathbf{a}^T \mathbf{x}) + \alpha \epsilon, \quad (37)$$



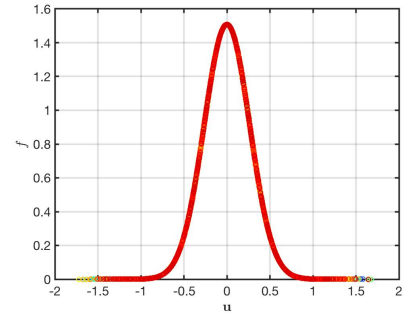
(a)



(b)



(c)



(d)

Figure 3: Results for the Gaussian ridge function where  $d = 5$  for  $N = 200$  in (a) and (c) and for  $N = 400$  in (b) and (d). Sub-figures (a) and (b) show the convergence history for the optimization, while sub-figures (c) and (d) show sufficient summary plots.

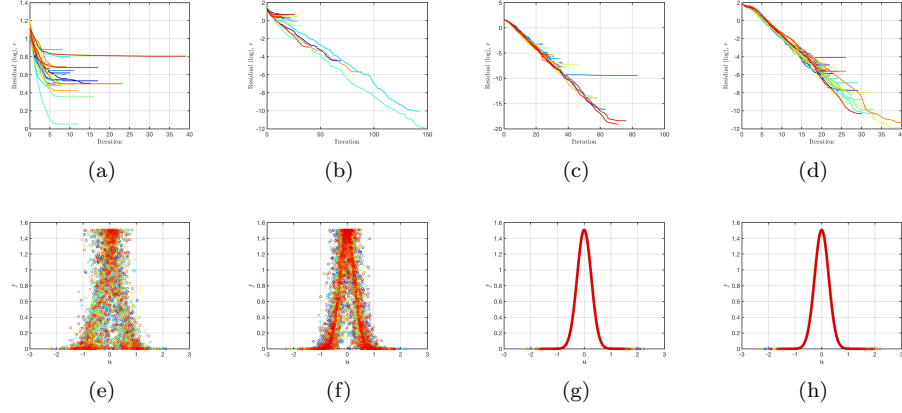


Figure 4: Results for the Gaussian ridge function where  $d = 100$  for  $N = 200$  in (a, e);  $N = 400$  in (b, f);  $N = 800$  in (c, g), and  $N = 1200$  in (d, h). The top row of sub-figures show the convergence history for the optimization, while the bottom row show the sufficient summary plots.

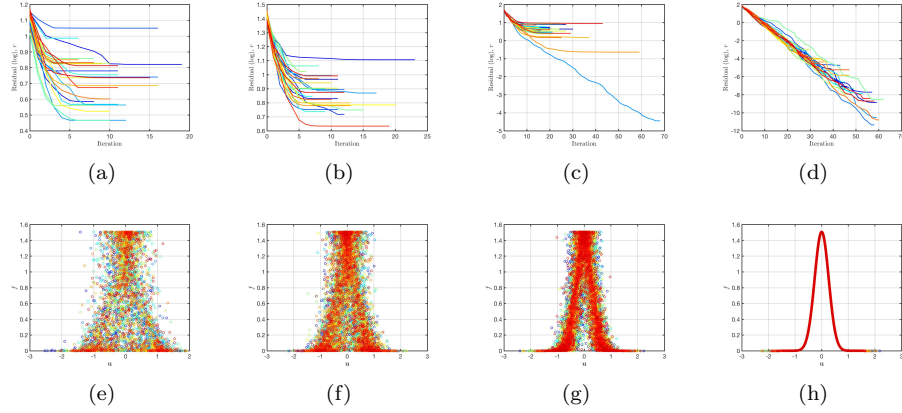


Figure 5: Results for the Gaussian ridge function where  $d = 200$  for  $N = 200$  in (a, e);  $N = 400$  in (b, f);  $N = 800$  in (c, g), and  $N = 1200$  in (d, h). The top row of sub-figures show the convergence history for the optimization, while the bottom row show the sufficient summary plots.



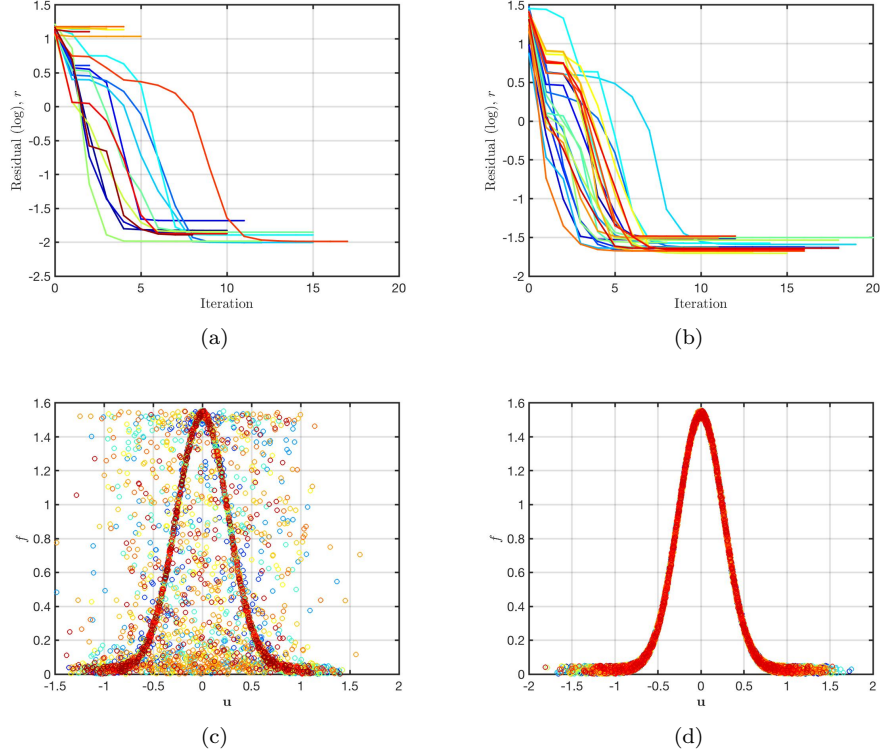


Figure 6: Results for the Gaussian ridge function where  $d = 5$  and  $\alpha = 0.05$  for  $N = 200$  in (a) and (c) and for  $N = 400$  in (b) and (d). Sub-figures (a) and (b) show the convergence history for the optimization, while sub-figures (c) and (d) show sufficient summary plots.

where  $\epsilon$  is a uniformly distributed random variable between 0 and 1 and  $\alpha$  is a scaling constant. In Figures 6 and 7 we show the results—using the convergence and sufficient summary plots as shown earlier—with  $\alpha = 0.05$  and  $\alpha = 0.10$  respectively. The results are shown for two values of  $N$ , i.e.,  $N = 200$  and  $N = 400$ .

While it is apparent that the addition of numerical noise drastically reduces the residuals, which is expected, the resulting sufficient summary plots do show that our algorithm is able to handle noisy function evaluations. This leads us to believe that it can be useful for problems rooted in statistical regression.

## 4.2 Turbomachinery case study

In this sub-section we use the turbomachinery case study considered in [33] to: compare the efficacy of our algorithm with a few SDR techniques. We make two key claims in this section for this turbomachinery case study: (a)

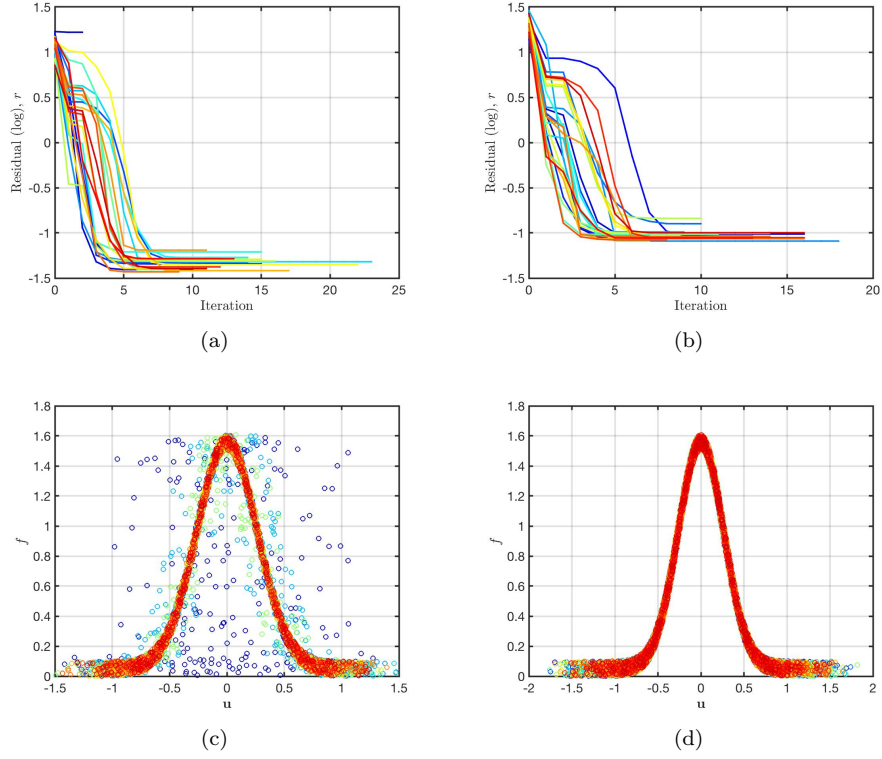


Figure 7: Results for the Gaussian ridge function where  $d = 5$  and  $\alpha = 0.10$  for  $N = 200$  in (a) and (c) and for  $N = 400$  in (b) and (d). Sub-figures (a) and (b) show the convergence history for the optimization, while sub-figures (c) and (d) show sufficient summary plots.

the standard deviation obtained from a Gaussian process may be used to make statements on the accuracy associated with the ridge approximation and (b) our algorithm achieves a lower predictive variance compared to four well-known sufficient dimension reduction methods: SIR, SAVE, MAVE and CR. To begin, we briefly summarize the turbomachinery case presented here.

In their work that investigates the use of active subspaces for learning turbomachinery aerodynamic pedigree rules of design, the authors in [33] parameterize an aero-engine fan fan with 25 design variables—five degrees of freedom defined at five spanwise locations. Once the geometry is generated, the mesh generation and flow solver codes described in [33] are used to solve the Reynolds average Navier Stokes equations (RANS) for the particular blade design; a post processing routine is then utilized for estimating the efficiency—our *quantity of interest*. In the aforementioned paper, the authors run a design of experiment with 548 different designs for estimating the active subspaces via a global quadratic model, which required estimating 351 polynomial coefficients. In what follows, we demonstrate the efficacy of our algorithm with far fewer samples.

We randomly (uniformly) select  $N = 300$  samples from the above DOE; input/output pairs  $(\mathbf{x}_i \in \mathbb{R}^{25}, f_i \in \mathbb{R})$  for  $i = 1, \dots, N$ . These samples are provided as inputs to SIR, SAVE, CR and MAVE for estimating a dimension reducing subspace. The computed subspaces  $\tilde{\mathbf{M}} \in \mathbb{R}^{d \times 2}$  are then used for generating sufficient summary plots and for fitting a Gaussian process regression response. To ensure parity, all methods use the same 300 samples.

To ascertain how appropriate the choice of a particular  $\tilde{\mathbf{M}}$  is, we use all 548 DOE points in the sufficient summary plots and in the Gaussian process regression (even though the subspaces  $\tilde{\mathbf{M}}$  are estimated with strictly 300 samples). Figures 8 (a) and (c) are the computed sufficient summary plots for SIR and SAVE. Here the vertical axis represents the normalized efficiency, while the horizontal axis for a particular design  $\mathbf{x}_i$  is given by

$$\mathbf{u}_1 = \left( \tilde{\mathbf{M}}(:, 1) \right)^T \mathbf{x} \quad \text{and} \quad \mathbf{u}_2 = \left( \tilde{\mathbf{M}}(:, 2) \right)^T \mathbf{x}, \quad (38)$$

where the notation  $(:, k)$  denotes the  $k$ -th column of  $\tilde{\mathbf{M}}$ . Figures 8 (c) and (d) show contours of the  $2\sigma$  values obtained from the Gaussian process response surface. Similar plots for CR and MAVE are shown in Figure 9. It is clear from these plots that MAVE and SIR yield lower  $2\sigma$  values on average. SAVE and CR fail to identify any low dimensional structure. In contrast the result of our algorithm is shown in Figure 10. The  $2\sigma$  contours shown in Figure 10 are by far the lowest and one can clearly see that all the data lies on a quadratic manifold.

## 5 Conclusion

In this paper we introduce a new algorithm for ridge function approximation tailored for subspace-based dimension reduction. Given point evaluations of a model, our algorithm approximates the ridge subspace  $\mathbf{M}$  by minimizing a quadratic form of the function and its best ridge approximation. Throughout

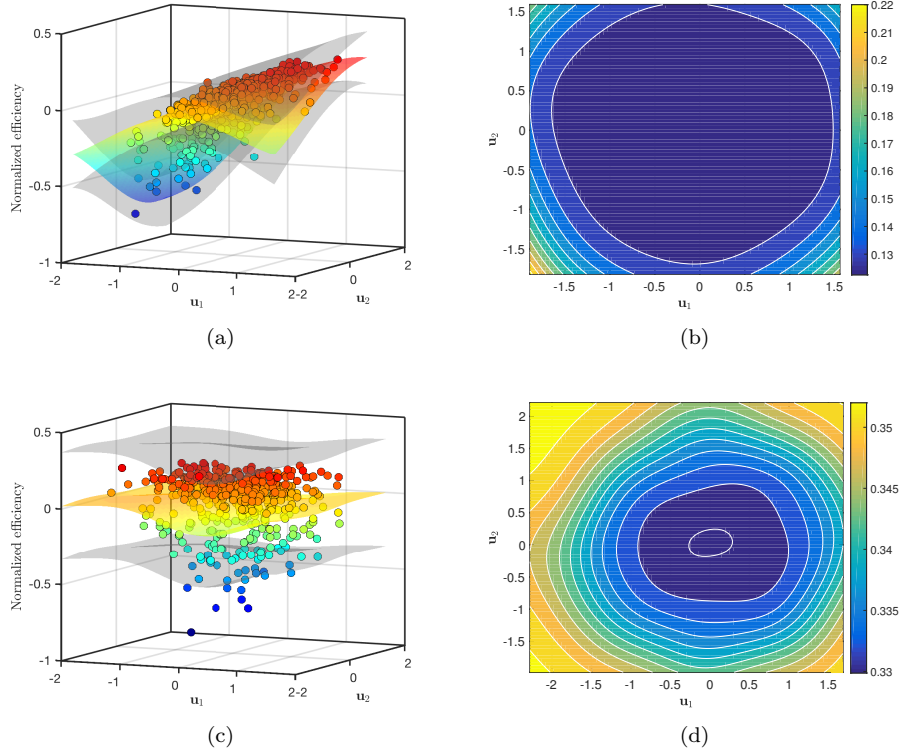


Figure 8: Turbomachinery case study results for estimating the ridge subspace followed by Gaussian process regression for estimating the mean and  $2\sigma$  response surfaces. Sufficient summary plots and  $2\sigma$  contours are shown here for (a, b) SIR and (c, d) SAVE.

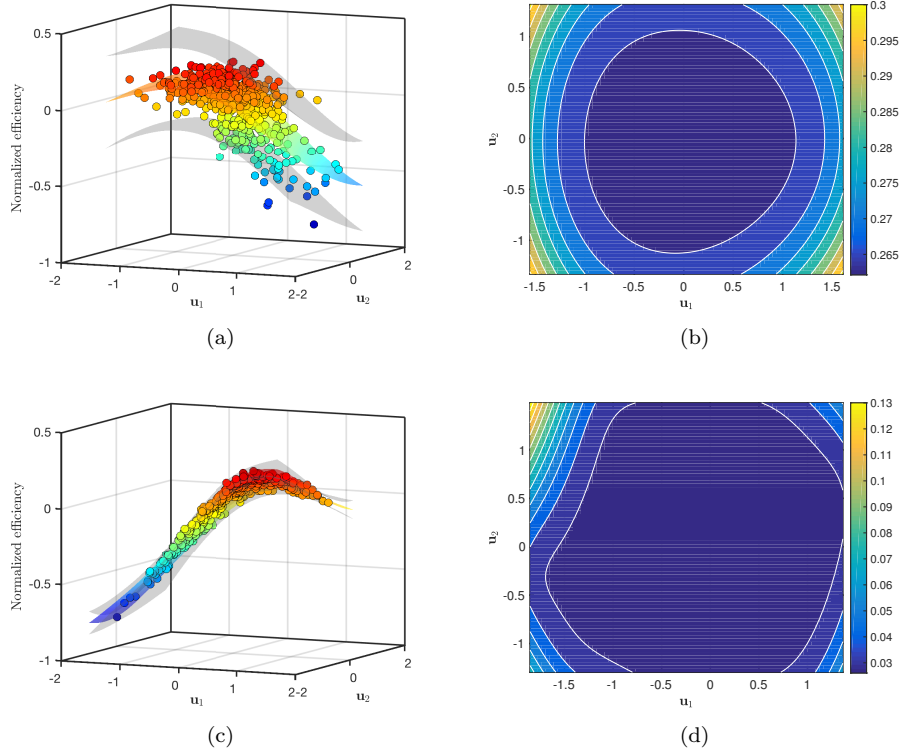


Figure 9: Turbomachinery case study results for estimating the ridge subspace followed by Gaussian process regression for estimating the mean and  $2\sigma$  response surfaces. Sufficient summary plots and  $2\sigma$  contours are shown here for (a, b) CR and (c, d) MAVE.

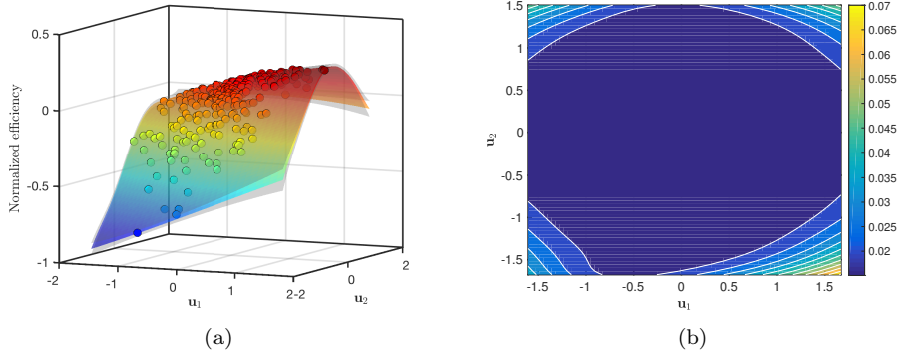


Figure 10: Turbomachinery case study results for estimating the ridge subspace followed by Gaussian process regression for estimating the mean and  $2\sigma$  response surfaces. Sufficient summary plots (a) and  $2\sigma$  contours (b) are shown here for our algorithm.

this paper, we assume our ridge function is the posterior mean of a Gaussian process. Our results for the examples considered demonstrate: (i) our algorithm is able to obtain near-exact recovery; (ii) our algorithm is robust to noisy function evaluations, and (iii) our algorithm offers better results compared with the four sufficient dimension reduction techniques considered in this paper.

## 6 Acknowledgements

The authors are grateful to Paul Constantine for insightful discussions. The first author would like to acknowledge the support of a Rolls-Royce fellowship. The second author would like to acknowledge the financial support of Magdalene College, Cambridge.

## References

- [1] P-A Absil, Robert Mahony, and Rodolphe Sepulchre. *Optimization algorithms on matrix manifolds*. Princeton University Press, 2009.
- [2] K. P. Adragni and R. D. Cook. Sufficient dimension reduction and prediction in regression. *Philosophical Transactions of the Royal Society A: Mathematical, Physical and Engineering Sciences*, 367(1906):4385–4405, 2009.
- [3] Nicolas Boumal, Bamdev Mishra, P.-A. Absil, and Rodolphe Sepulchre. Manopt, a matlab toolbox for optimization on manifolds. *Journal of Machine Learning Research*, 15:1455–1459, 2014.

- [4] Albert Cohen, Ingrid Daubechies, Ronald DeVore, Gerard Kerkyacharian, and Dominique Picard. Capturing ridge functions in high dimensions from point queries. *Constructive Approximation*, 35(2):225–243, 2012.
- [5] Paul Constantine and David Gleich. Computing active subspaces with monte carlo. *arXiv preprint arXiv:1408.0545*, 2014.
- [6] Paul G Constantine. *Active subspaces: Emerging ideas for dimension reduction in parameter studies*. SIAM, 2015.
- [7] Paul G Constantine, Eric Dow, and Qiqi Wang. Active subspace methods in theory and practice: applications to kriging surfaces. *SIAM Journal on Scientific Computing*, 36(4):A1500–A1524, 2014.
- [8] Paul G. Constantine, Armin Eftekhari, Jeffrey Hokanson, and Rachel A. Ward. A near-stationary subspace for ridge approximation. *Computer Methods in Applied Mechanics and Engineering*, 326(Supplement C):402 – 421, 2017.
- [9] Paul G Constantine, Brian Zaharatos, and Mark Campanelli. Discovering an active subspace in a single-diode solar cell model. *Statistical Analysis and Data Mining: The ASA Data Science Journal*, 8(5-6):264–273, 2015.
- [10] R. D. Cook. Save: a method for dimension reduction and graphics in regression. *Communications in statistics-Theory and methods*, 29(9-10):2109–2121, 2000.
- [11] R. D. Cook. *Regression graphics: Ideas for studying regressions through graphics*, volume 482. John Wiley & Sons, 2009.
- [12] R. D. Cook and L. Ni. Sufficient dimension reduction via inverse regression: A minimum discrepancy approach. *Journal of the American Statistical Association*, 100(470):410–428, 2005.
- [13] R. Dennis Cook. Rejoinder: Fisher Lecture: Dimension Reduction in Regression. *Statistical Science*, 22(1):40–43, 2007.
- [14] R. Dennis Cook and Liqiang Ni. Sufficient dimension reduction via inverse regression: A minimum discrepancy approach. *Journal of the American Statistical Association*, 100(470):410–428, 2005.
- [15] Paul Diaz, Paul Constantine, Kelsey Kalmbach, Eric Jones, and Stephen Pankavich. A modified {SEIR} model for the spread of ebola in western africa and metrics for resource allocation. *Applied Mathematics and Computation*, 324:141 – 155, 2018.
- [16] Alan Edelman, Tomás A Arias, and Steven T Smith. The geometry of algorithms with orthogonality constraints. *SIAM Journal on Matrix Analysis and Applications*, 20(2):303–353, 1998.

- [17] Massimo Fornasier, Karin Schnass, and Jan Vybiral. Learning functions of few arbitrary linear parameters in high dimensions. *Foundations of Computational Mathematics*, 12(2):229–262, 2012.
- [18] J. Friedman, T. Hastie, and R. Tibshirani. *The elements of statistical learning*, volume 2. Springer series in statistics New York, 2008.
- [19] A. T Glaws and R. D. Constantine, P. G. and Cook. Inverse regression for ridge recovery. *arXiv preprint arXiv:1702.02227*, 2017.
- [20] Gene H Golub and Charles F Van Loan. *Matrix computations*, volume 4. JHU Press, 2013.
- [21] Zach Grey and Paul Constantine. *Active Subspaces of Airfoil Shape Parameterizations*. American Institute of Aeronautics and Astronautics, 2018/01/02 2017.
- [22] Bing Li and Shaoli Wang. On directional regression for dimension reduction. *Journal of the American Statistical Association*, 102(479):997–1008, 2007.
- [23] K. C. Li. Sliced inverse regression for dimension reduction. *Journal of the American Statistical Association*, 86(414):316–327, 1991.
- [24] Xiaoyu Liu and Serge Guillas. Dimension reduction for gaussian process emulation: an application to the influence of bathymetry on tsunami heights. *SIAM/ASA Journal on Uncertainty Quantification*, 5(1):787–812, 2017.
- [25] Yanyuan Ma and Liping Zhu. A review on dimension reduction. *International Statistical Review*, 81(1):134–150, 2013.
- [26] Luca Magri, Michael Bauerheim, Franck Nicoud, and Matthew P Juniper. Stability analysis of thermo-acoustic nonlinear eigenproblems in annular combustors. part ii. uncertainty quantification. *Journal of Computational Physics*, 325:411–421, 2016.
- [27] Allan Pinkus. *Ridge functions*, volume 205. Cambridge University Press, 2015.
- [28] Elijah Polak. *Optimization: algorithms and consistent approximations*, volume 124. Springer Science & Business Media, 2012.
- [29] Friedrich Pukelsheim. *Optimal design of experiments*, volume 50. siam, 1993.
- [30] Carl Edward Rasmussen and Hannes Nickisch. Gaussian processes for machine learning (gpml) toolbox. *Journal of Machine Learning Research*, 11(Nov):3011–3015, 2010.



- [31] Carl Edward Rasmussen and Christopher KI Williams. *Gaussian processes for machine learning*, volume 1. MIT press Cambridge, 2006.
- [32] Alexander M Samarov. Exploring regression structure using nonparametric functional estimation. *Journal of the American Statistical Association*, 88(423):836–847, 1993.
- [33] Pranay Seshadri, Shahrokh Shahpar, Paul Constantine, Geoffrey Parks, and Mike Adams. Turbomachinery active subspace performance maps. *Journal of Turbomachinery*, 140(4):041003–11, 01 2018.
- [34] Rohit Tripathy, Ilias Bilonis, and Marcial Gonzalez. Gaussian processes with built-in dimensionality reduction: Applications to high-dimensional uncertainty propagation. *Journal of Computational Physics*, 321:191–223, 2016.
- [35] Hemant Tyagi and Volkan Cevher. Learning non-parametric basis independent models from point queries via low-rank methods. *Applied and Computational Harmonic Analysis*, 37(3):389–412, 2014.
- [36] Yingcun Xia, Howell Tong, WK Li, and Li-Xing Zhu. An adaptive estimation of dimension reduction space. *Journal of the Royal Statistical Society: Series B (Statistical Methodology)*, 64(3):363–410, 2002.
- [37] Li-Ping Zhu and Li-Xing Zhu. Dimension reduction for conditional variance in regressions. *Statistica Sinica*, pages 869–883, 2009.